

Deactivation Dynamics of Rough Catalytic Surfaces

M. Filoche and B. Sapoval

Laboratoire de Physique de la Matière Condensée, C.N.R.S. Ecole Polytechnique, 91128 Palaiseau, France, and Centre de Mathématiques et de leurs Applications, Ecole Normale Supérieure, 94140 Cachan, France

J. S. Andrade, Jr.

Laboratoire de Physique de la Matière Condensée, C.N.R.S. Ecole Polytechnique, 91128 Palaiseau, France; Departamento de Física, Universidade Federal do Ceará, Brazil, and Programa de Pós-Graduação em Engenharia Química, Universidade Federal do Ceará, 60451-970 Fortaleza, Ceará, Brazil

DOI 10.1002/aic.10366

Published online in Wiley InterScience (www.interscience.wiley.com).

The dynamics of deactivation due to parallel fouling is investigated in the case of a rough reactive interface under diffusion-limited conditions. For a first-order reaction, a mathematical method is introduced that permits to analyze the response of the system for any type of interface geometry or input condition. Exact analytical results, such as the lifetime of the catalyst or its total production are calculated. The deactivation dynamics in specific geometries, such as a flat catalytic surface, an infinite pore or a rough surface, are examined. Through these three examples, a general picture of the role of the morphology on the system response is provided. Even more, this approach shows that the determination of a single time response function of a catalyst of unknown morphology provides a means to control the dynamics of the production process. © 2005 American Institute of Chemical Engineers *AIChE J*, 51: 998–1008, 2005

Keywords: catalysis, computer simulations, diffusion, mass transfer

Introduction

The understanding of heterogeneous catalysis today represents an important economic and scientific challenge. The development of techniques for the preparation and/or selection of catalyst materials constitutes an important aspect of this subject. From a theoretical point of view, some research effort in recent years has been dedicated to model catalytic systems under a more realistic geometrical framework. For instance, it is well known that the classical pseudo-homogeneous models for the description of the diffusion-reaction process in porous catalysts^{1,2} can only implicitly account for the geometrical features of real pore spaces.^{3,4} The standard modeling approach indeed considers the catalyst particle as a homogeneous system

where reactants and products can diffuse (molecular or Knudsen diffusion), and react according to a given effective transport coefficient and an intrinsic reaction mechanism. One characteristic of heterogeneous catalysis that deserves special attention is the progressive decrease in time of the surface activity. The cost involved in catalyst replacement and process shutdown for the industry due to deactivation can be extremely high, reaching the order of billions of dollars per year.

Generally speaking, the effect of the porous geometry on the reactive properties of catalysts has been investigated with a great variety of irregular structures (for example, pore trees, pore networks, surface of fractal aggregates and fractal pore spaces).^{5–10} At the pore level, the role played by the local surface morphology on the overall efficiency of the catalyst has also been the subject of previous studies.^{11–15} The fractal concept, in particular, has been adopted as a model for the surface geometry of some disordered materials, including catalyst supports and adsorbents.¹⁶ The effect of the nonuniform accessi-

Correspondence concerning this article should be addressed to M. Filoche at marcel.filoche@polytechnique.fr.

bility of the active sites on the reactivity of irregular catalyst surfaces is a subject of great interest in heterogeneous catalysis. Due to *screening* effects, even if one assumes that the active sites are uniformly distributed in space along the surface, the deep parts of the structure may still display a lower activity when compared to the most exposed regions of the catalyst. As a result, the efficiency of the catalyst surface can be substantially different than the one expected from the intrinsic chemical reactivity.

The extensive research developed in the last years on the subject of linear transport through irregular interfaces has been mainly devoted to the introduction, calculation, and application of the concept of *active zone*.^{17–19} Inspired by this idea, a new coarse-graining method has been proposed¹⁷ to calculate the flux through irregular surfaces from their geometry alone, without solving the general Laplace problem. More recently^{20,21} the notion of active zone has been extended to reactive interfaces of arbitrary shape. It has been shown, by direct numerical simulation, that the coarse graining technique presented in Sapoval¹⁷ provides consistent predictions for the activity of catalyst surfaces over a wide range of diffusion-reaction conditions (that is, with or without screening effects). In many practical cases, the effect of roughness is to increase the intrinsic reaction rate by a geometrical factor, namely, the ratio between the real and the apparent surface area. Here, we are implicitly assuming that the active sites are uniformly distributed in space along the entire surface. This is not necessarily true for all catalytic systems. For example, the impregnation process of a rough catalyst substrate may result in a highly dispersed distribution of active sites that can substantially reduce the catalyst activity.

Catalyst deactivation during the campaign of a chemical reactor is often impossible to avoid. The dynamical characteristics of this phenomenon should, therefore, be carefully considered in the design of the diffusion-reaction system, as well as in the process operation and optimization strategies.²² The deactivation time, however, can vary over a wide range of time scales. Most of the catalysts of technological importance deactivate because of poisoning, sintering, and fouling or coke formation.^{23,24} The term poisoning refers to the loss of catalytic activity due to strong chemisorption or reaction of a chemical impurity with the active sites, preventing their access by the reagent species. If sintering occurs, normally due to high temperatures in the system, the activity loss might result from the decrease in the effective catalytic surface area. Finally, in the case of coking or fouling, the decrease in activity is a consequence of the formation of solid products (for example, carbonaceous residues) which deposit on the surface of the catalyst and impair its reactive efficiency. In a later stage, apart from a decrease in the available active surface, the formation of coke can produce drastic changes in the pore space volume and connectivity due to physical pore plugging.

The modeling of catalyst deactivation has been recently addressed by Froment²⁵ with emphasis on the mechanism of coke formation. Accordingly, this should be viewed as a three-fold problem, where the microscopic scale of the active site, the level of the catalyst particle, and the more macroscopic features of a chemical reactor operation have to be considered. At the level of the catalyst pellet, in particular, the role played by the geometry of the pore space on the dynamics of the deactivation process has been the focus of some previous studies.^{26–29} A

close analogy between catalyst deactivation and percolation processes has been suggested by Sahimi and Tsotsis,³⁰ where a special type of percolation model with *trapping* is developed to describe the effect of the porous media interconnectedness on the accessibility of individual pores to transport and chemical reaction. In a subsequent work, Arbabi and Sahimi^{31,32} developed a model of deactivation for heterogeneous catalysis, based on a network representation of the pore geometry. As a paradigm for catalytic pore plugging, this certainly represents a more realistic approach because phenomenological and structural features of the system are considered in the same theoretical framework.

If we now consider that the catalyst interface is slowly deactivating due to a fouling mechanism, the following interesting question arises naturally: what is the role of the roughness geometry on the dynamics of the deactivation process? Furthermore and more important, how do the geometry and the deactivation process combine to affect the overall performance and duration of the catalytic activity? The aim of the present study is to give some preliminary answers to these questions. The most important result of our theoretical work is to suggest a new way to control the time dependence of the catalytic production under slow deactivation. For a first-order reaction, our results show that *the knowledge of a single time response function of the system provides a means to control the production process under a broad range of operational conditions. Moreover, we show that this general result can be applied to a catalyst of unknown deactivation dynamics and arbitrary geometry.* As an example, we present in this article a numerical experiment through the case study of a fractal catalytic surface.

This article is organized as follows. In the section titled “Theoretical Model,” we describe the catalytic system, and the deactivation model of parallel fouling studied here. We show that a mathematical analysis of this model allows to map the dynamics of diffusion, reaction and deactivation into a steady-state problem, but with a nonlinear boundary condition at the catalytic surface. Some general exact results that do not depend on the shape of the catalytic surface are then presented in the section titled “Results.” In particular, it is shown that the total integrated production of a progressively deactivated catalyst is exactly proportional to its developed area. In the section titled “Examples of Catalytic Interfaces,” several paradigmatic shapes of interfaces are studied in order to get a general understanding of the link between the geometrical features of the catalytic interface and the overall response of the catalytic cell. At last, in the section titled “Controlling the Time Production of an Unknown Catalyst,” a new way of accessing the microscopic properties of the interface and, at the same time, to control the output flux of the system, are proposed.

Theoretical Model

Reaction kinetics of parallel fouling

We first introduce the model describing the slow deactivation of an irregular catalytic surface in the Eley-Rideal situation. In such a system, the bulk diffusion of the reactant A towards the catalytic surface is described by Fick’s law, $\vec{J}_A = -D\vec{\nabla}C_A$, where C_A is the concentration and D is the diffusion coefficient of species A . When encountering the surface, a molecule A can react in two different ways. First, it can react with the catalytic species X to create a new species A^*

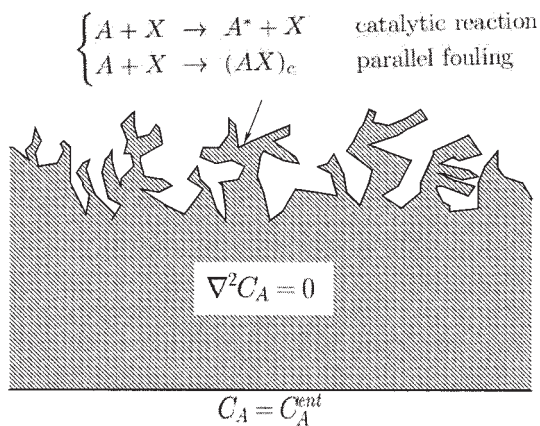


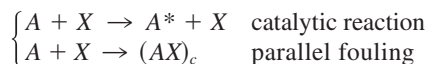
Figure 1. Chemical reactions involved in parallel fouling.



Along with this process, a second reaction can also take place creating the complex species $(AX)_c$. In this new state, the species X is no longer active as a catalyst. This mechanism, called *parallel fouling*, thus, deactivates the catalyst X according to



As depicted in Figure 1, we are concerned with the steady-state regime of the system



where the concentration C_A in the bulk of the diffusion-reaction cell obeys the Laplace equation

$$\nabla^2 C_A = 0 \quad (3)$$

The use of Laplace equation implies that the discussion which follows should be limited to mass transport by molecular diffusion. This is justified here by assuming that the effects of the micro-roughness linked to the Knudsen diffusion mechanism can be included in the reaction rates values, coarse-grained to a length scale of the order of the molecular mean free path.^{20,21} The molecular mean free path, therefore, constitutes the lower cut-off for the validity of our description. For example, Knudsen diffusion (instead of molecular diffusion) may become the dominant mechanism of mass transport determining the reactivity of the system if the reagent is a diluted gas for which the collisions among molecules are less frequent than the collisions between the molecules and the catalytic surface.^{11,15,33,34}

On the catalytic surface, the local flux of disappearance of species A is given by

$$j = k_1 C_X C_A + k_2 C_X C_A = K C_X C_A \quad (4)$$

where C_X is the surface concentration of active sites, k_1 and $k_2 \ll k_1$ are the rate coefficients for the catalytic and the deac-

tivation reactions, respectively, and $K = k_1 + k_2$. While the boundary condition at the catalytic surface is given by

$$D \frac{\partial C_A}{\partial n} = K C_X C_A, \quad (5)$$

the local rate of catalyst concentration C_X decreases due to the kinetics of the parallel fouling as

$$\frac{dC_X}{dt} = -k_2 C_X C_A. \quad (6)$$

The dynamics of the species A and X are then described by the following set of equations

$$\begin{cases} C_A = C_A^{ent}(t) & \text{at the source} & (a) \\ \nabla^2 C_A = 0 & \text{in the bulk} & (b) \\ \frac{\partial C_A}{\partial n} = \frac{K}{D} C_X(\vec{x}, t) C_A(\vec{x}, t) & \text{at the surface} & (c) \\ \frac{dC_X}{dt} = -k_2 C_X(\vec{x}, t) C_A(\vec{x}, t) & \text{at the surface} & (d) \end{cases} \quad (7)$$

As explained later, the concentration of A at the source, C_A^{ent} , can be time-dependent and used as a control variable for the production of the system.

In the particular case of a constant concentration of A at the source, the evolution of $C_A(\vec{x}, t)$ is solely due to the variation of the concentration of active catalyst on the surface. Equations 7 represent a nonlinear system with two unknowns C_A and C_X , which has no analytical solution. It will be shown that, from a convenient integral transformation, this problem can be treated as a nonlinear steady-state system with a single unknown, that can be studied mathematically.

Steady-state formulation

We first introduce the time-integrated concentration of species A , $I(\vec{x}, t)$, defined everywhere in the system as

$$I(\vec{x}, t) \equiv \int_0^t C_A(\vec{x}, \tau) d\tau \quad (8)$$

As a linear function of $C_A(\vec{x}, t)$, this quantity also obeys the Laplace equation, $\nabla^2 I = 0$. We now show that our dynamical system can be mapped in terms of the diffusion-reaction behavior of the single variable I , with a nonlinear boundary condition on the catalytic surface. For this, Eq. 7d can be directly integrated with respect to time to give

$$C_X(\vec{x}, t) = C_X^0(\vec{x}) e^{-k_2 I(\vec{x}, t)} \quad (9)$$

where $C_X^0(\vec{x})$ is the initial distribution of active sites on the surface at time $t = 0$. The boundary condition for I at the catalytic surface is then obtained from the combination of Eqs. 7c and 7d and integration in time

$$\frac{\partial I}{\partial n} = \left(\frac{1 - e^{-k_2 I}}{k_2 I} \right) \frac{I}{\Lambda_0(\vec{x})}$$

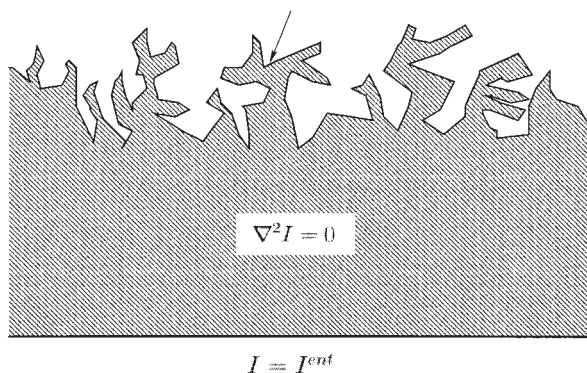


Figure 2. Steady-state nonlinear problem in terms of the time-integrated concentration $I(\vec{x}, t)$.

$$\frac{\partial I}{\partial n} = \int_0^t \frac{\partial C_A(\vec{x}, \tau)}{\partial n} d\tau = - \int_0^t \frac{K}{Dk_2} \frac{dC_X}{dt} d\tau \quad (10)$$

leading to

$$\frac{\partial I}{\partial n} = \frac{KC_X^0(\vec{x})}{Dk_2} [1 - e^{-k_2 I}] \quad (11)$$

As a result, the deactivation problem can be formulated by means of the following set of equations

$$\begin{cases} I = I^{ent} = \int_0^t C_A^{ent}(\tau) d\tau & \text{at the source} & (a) \\ \nabla^2 I = 0 & \text{in the bulk} & (b) \\ \frac{\partial I}{\partial n} = \frac{1 - e^{-k_2 I}}{k_2 \Lambda_0(\vec{x})} & \text{at the surface} & (c) \end{cases} \quad (12)$$

with

$$\Lambda_0(\vec{x}) \equiv \frac{D}{KC_X^0(\vec{x})} \quad (13)$$

$$\frac{\partial I}{\partial n} = \left(\frac{1 - e^{-k_2 I}}{k_2 I} \right) \frac{I}{\Lambda_0(\vec{x})}$$

where the diffusion-reaction system is described only in terms of the new variable I . Time is now a dummy variable which only appears through the boundary condition at the source. For a fixed value of I^{ent} , this set of equation represents a nonlinear steady-state system. See Figure 2.

At early times, $I \approx 0$ everywhere, and Λ_0 appears as the relevant parameter ruling the mixed boundary condition 12c. Previous works have shown that this parameter can be interpreted as the size of a subset of the catalytic interface that works uniformly.^{17,35}

From the solution of the steady state system Eqs. 12, the evolution of the dynamical system can be obtained in the

following way: let $\Phi(I^{ent})$ be the response of the nonlinear system 12

$$\Phi(I^{ent}) = -D \int_{surf.} \frac{\partial I}{\partial n} ds \quad (14)$$

We are interested in the time-dependent flux of A species that can be written as

$$\phi_A(t) = -D \int_{surf.} \frac{\partial C_A}{\partial n} ds \quad (15)$$

From the definition 8 and using Eqs. 14 and 15, the flux ϕ_A relates to the response Φ by means of a simple time derivative

$$\phi_A(t) = -D \int_{surf.} \frac{\partial}{\partial n} \frac{\partial I}{\partial t} ds = \frac{d}{dt} [\Phi(I^{ent}(t))] = \frac{dI^{ent}}{dt} \frac{d\Phi(I^{ent})}{dI^{ent}} \quad (16)$$

The resulting Eq. 16 expresses mathematically the fact that, if the solution $\Phi(I^{ent})$ is known for any I^{ent} , one can predict the dynamic response of the system for any arbitrary, and even time-dependent, input concentration $C_A^{ent}(t)$. Therefore, we can call the function $\Phi(I^{ent})$ the “master curve” of the system. It is important to stress that this curve also gives the cumulative production at time t as a function of the integrated entrance concentration. Moreover, this result is valid whatever the variation in time of concentration at the source.

For completeness, the flux of product A^* is given by

$$\phi_{A^*}(t) = \frac{k_1}{K} \phi_A(t) \quad (17)$$

and since $k_2 \ll k_1$, we can assume that, for all practical purposes

$$\phi_{A^*} \approx \phi_A \quad (18)$$

Results

Constant concentration at the source

For a constant concentration at the source C_A^{ent} , the flux of A through the catalytic surface becomes

$$\phi_A(t) = C_A^{ent} \left. \frac{d\Phi}{dI^{ent}} \right|_{(I^{ent}=C_A^{ent}t)} \quad (19)$$

This equation indicates that the time dependency of the production provides a direct way to determine the function $d\Phi/dI^{ent}$ of a catalytic system that, in general, is not known *a priori*. As we will show in the subsection titled “The case of prefractal interfaces”, this single function contains the signatures of the geometrical, as well as the physicochemical characteristics of the catalytic system, namely, the internal geom-

entry of the interface, the distribution of active sites, the diffusivity, and both the reaction and fouling kinetics.

Total production of the catalytic system

Using the approximation 18 the total catalytic production can be written as

$$N = \int_0^{+\infty} \phi_A(t) dt \quad (20)$$

The time integrated flux of A is the flux of I when $t \rightarrow +\infty$. In this limit, I increases everywhere, and the boundary condition 11 saturates at the value $(KC_X^0(\vec{x})/k_2D)$. This leads to

$$N = \frac{k_1}{k_2} \int_{surf.} C_X^0(\vec{x}) ds \quad (21)$$

The production of A^* molecules is then directly determined by the total amount of available catalyst, with or without diffusion limitations, and *independently of the interface morphology*. In the case of a uniform distribution of catalyst, C_X^0 , N is simply proportional to S_{tot}

$$N = \left(\frac{k_1 C_X^0}{k_2} \right) S_{tot} \quad (22)$$

where $S_{tot} (= \int_{surf.} ds)$ is the total developed surface of the catalyst.

Time response in the absence of diffusion limitation

For sufficiently large diffusivity or, equivalently, small enough systems, the concentration of A is uniform everywhere and equal to C_A^{ent} . In this situation

$$C_X(\vec{x}, t) = C_X^0(\vec{x}) e^{-k_2 C_A^{ent} t} \quad (23)$$

and, from Eq. 4, the flux is given by

$$\phi_A = (KC_X^0 C_A^{ent}) \exp\left(-\frac{t}{\tau_0}\right) \quad (24)$$

where

$$\tau_0 \equiv (k_2 C_A^{ent})^{-1} \quad (25)$$

τ_0 is the intrinsic characteristic time of the deactivation process. This typical time constant of deactivation may be experimentally determined by monitoring the deactivation of a sufficiently small catalyst pellet.

Examples of Catalytic Interfaces

As already mentioned, under diffusion-limited conditions, screening effects can have an important role on the overall performance of the catalytic interface.^{36,37,38} One possible way

to quantify the influence of the shape of the interface on the response of the diffusion-reaction cell is to characterize the irregularity of the geometrical interface in terms of the screening ratio³⁹

$$S \equiv L_p/L \quad (26)$$

where L and L_p are the size of the cell and the perimeter of the interface, respectively. In the following subsections, we investigate the deactivation behavior of three systems whose morphologies correspond to distinct values of the parameter S . Precisely, we study the case of the flat interface, for which $S = 1$, the infinite pore, for which $S \rightarrow \infty$, and at last, a set of prefractal interfaces whose generations rank from 0 to 5, and for which S takes finite values ranging from 1 to more than 4. For simplicity, we assume in all cases that the initial distribution of catalyst concentration C_X ($t = 0$) is uniform at the interface. This implies that the parameter Λ_0 is identical at every point of the catalytic surface. Also, the source concentration of C_A at the source, C_A^{ent} , is kept constant in time.

Flat catalytic surface

For a flat interface, the problem is essentially one-dimensional (1-D). Since I obeys the Laplace equation, the gradient of I is constant in the bulk. Let I^{su} be the value of I at the surface, and h the distance between the source and the catalytic surface (the height of the cell). Equating the flux of I both at the catalytic surface and in the bulk, yields the following relation

$$S_{tot} \left(\frac{KC_X^0}{k_2} \right) [1 - e^{-k_2 I^{su} t}] = \frac{S_{tot} D}{h} (I^{ent} - I^{su}) \quad (27)$$

The term on the right of this equation is the flux of I across the cell, and its time derivative is then the flux of A . Writing the derivative of the left term one obtains

$$\phi_A = (KC_X^0) e^{-k_2 I^{su} t} \frac{dI^{su}}{dt} S_{tot} \quad (28)$$

Although Eq. 27 cannot be solved analytically, it is possible to examine the behavior of the system both at the beginning and at longer times. Initially, at $t = 0$, $I^{ent} = I^{su} = 0$. As long as $k_2 I^{su} \ll 1$, Eq. 27 can be solved at first-order, which yields

$$I^{su} \approx \frac{I^{ent}}{1 + \frac{h}{\Lambda_0}} \quad \text{and} \quad \phi_A \approx \frac{DC_A^{ent}}{h + \Lambda_0} S_{tot}$$

Λ_0 being the length introduced in Eq. 13. During this first period, the flux of A is constant. It means that the catalyst has not been significantly altered by the fouling process, which is slowed down by diffusion. On the other hand, if $k_2 I^{su} \gg 1$, Eq. 27 and Eq. 28 yield

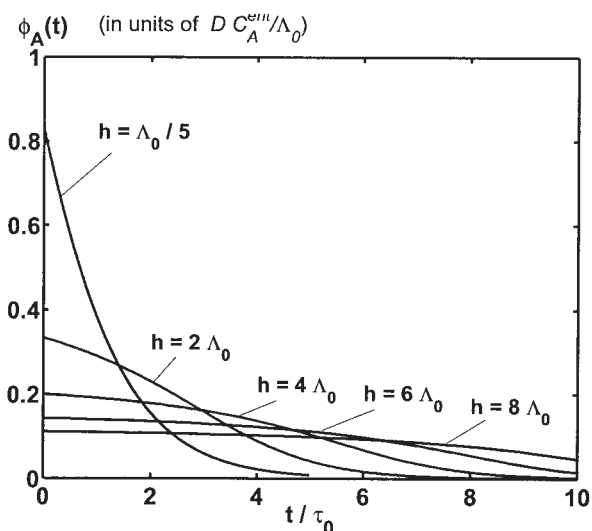


Figure 3. Chemical activity as a function of time for systems with a flat catalytic interface and various values of the height h : the integral under the different curves are the same.

$$\begin{cases} I^{su} \approx I^{ent} - \frac{h}{\Lambda_0 k_2} \\ \phi_A \approx \frac{S_{tot} D C_A^{ent}}{\Lambda_0} \exp\left(\frac{h}{\Lambda_0}\right) e^{-(t/\tau_0)} \end{cases} \quad (29)$$

The crossover condition between the short and long time regimes, $k_2 I^{su} \approx 1$, corresponds to

$$I^{ent} \approx \frac{1}{k_2} \left(1 + \frac{h}{\Lambda_0}\right)$$

which can be written as

$$t \approx \tau_0 \left(1 + \frac{h}{\Lambda_0}\right) \equiv \tau_1$$

This time τ_1 is the characteristic time of the deactivation process in the entire system, taking into account both the diffusion process through the cell of height h , and the deactivation process on the catalytic surface. It is interesting to note that the length h appears in the expression of the time as the diffusion across the cell commands the intensity of the fouling flux. In order to observe both times τ_0 and τ_1 , the solutions of Eq. 27 have been computed numerically. The time response of a flat catalytic surface for different values of h is shown in Figure 3.

In summary, the flux of reactants A through a cell with a flat catalytic surface remains constant, at a value $DS_{tot}C_A^{ent}/(h + \Lambda_0)$, until $t = \tau_1$. After this time, Eq. 29 shows that the flux then decreases exponentially with a characteristic time τ_0 . In the case of an irregular interface with a distribution of distances between the source and the different regions of the surface, there will be corresponding different deactivation times, as discussed in the section titled “The case of prefractal interfaces.”

The infinite pore

In the geometry of an infinite pore (in 2 or 3 dimensions), the steady-state system 12 can be transformed into a 1-D differential equation, where x is the abscissa along the pore, and $\tilde{I}(x, t)$ is the mean of $I(x, y, z, t)$ over the cross section of the pore. This unknown obeys

$$\frac{d^2 \tilde{I}}{dx^2} = \left(\frac{p}{\sigma}\right) \frac{1 - e^{-k_2 \tilde{I}}}{k_2 \Lambda_0} \quad (30)$$

where $\tilde{I}(x = 0, t) = C_A^{ent} t$ and (p/σ) is the ratio between the perimeter and the area of the cross section of the pore (in two dimensions, this parameter is equal to $2/w$, where w is the width of the pore). The second term of Eq. 30 is simply proportional (with a factor $D\sigma$) to the flux density of \tilde{I} per unit length along the pore.

After solving Eq. 30, the time-integrated concentration \tilde{I} and its flux Φ_I along the pore can be expressed as

$$\tilde{I}(x, t) = \frac{1}{k_2} g \left[f\left(\frac{t}{\tau_0}\right) - \frac{x}{\ell_c} \right] \quad (31)$$

$$\Phi_I(x, t) = \left(\frac{Dp}{\Lambda_0}\right) C_A^{ent} \tau_0 (1 - e^{-k_2 \tilde{I}}) \quad (32)$$

where the length $\ell_c = \sqrt{\sigma \Lambda_0 / p}$, and the functions f and g are defined by

$$f(u) = \int_1^u \frac{dv}{\sqrt{2(v + e^{-v} - 1)}} \quad \text{and} \quad g[f(u)] = u$$

From Eq. 32 one can immediately deduce the expressions of the concentration and the flux of A along the pore:

$$C_A(x, t) = C_A^{ent} \frac{f'\left(\frac{t}{\tau_0}\right)}{f'\left[g\left(f\left(\frac{t}{\tau_0}\right) - \frac{x}{\ell_c}\right)\right]} \quad (33)$$

$$\phi_A(x, t) = \left(\frac{Dp}{\Lambda_0}\right) C_A(x, t) e^{-g[f(t/\tau_0) - (x/\ell_c)]} \quad (34)$$

Finally, the total flux of reactants through the cell at time t can be exactly computed as

$$\phi_A(t) = \int_0^{+\infty} \phi_A(x, t) dx = \left(\frac{Dp C_A^{ent} \ell_c}{\Lambda_0 \sqrt{2}}\right) \frac{1 - e^{-t/\tau_0}}{\sqrt{t/\tau_0 + e^{-t/\tau_0} - 1}} \quad (35)$$

One then can see that the flux of a cell constituted by an infinite pore of perimeter p and cross section σ decreases as the inverse square root of time when t is much larger than τ_0

$$\phi_A(t) \approx DC_A^{ent} \sqrt{\frac{p\sigma}{2\Lambda_0}} \left(\frac{t}{\tau_0}\right)^{-(1/2)} \quad (36)$$

Early and Long Time Asymptotics. The expressions in Eqs. 33, 34 may look rather complicated, but the system behavior for early and late times for a given abscissa x can be investigated by considering the asymptotics of f

$$\begin{cases} \text{for } u \ll 1, f'(u) \approx \frac{1}{u} \text{ and } f(u) \approx \ln(u) \\ \text{for } u \gg 1, f'(u) \approx \frac{1}{\sqrt{2u}} \text{ and } f(u) \approx \sqrt{2u} \end{cases}$$

Let us first examine the early time behavior: for a given abscissa x in the pore, as long as $t \ll \tau_0$, then

$$C_A(x, t) \approx C_A^{ent} \exp\left(-\frac{x}{\ell_c}\right) \quad (37)$$

The concentration profile into the pore at the beginning is exponential with a characteristic length determined by both the geometry of the pore and the parameters governing the chemical reactions.

The long time asymptotics for a given abscissa x (larger than ℓ_c) is reached when the following condition is fulfilled

$$t \gg \frac{\tau_0}{2} \left(1 + \frac{x}{\ell_c}\right)^2$$

This represents the time for the fouling reaction to consume most of the catalyst up to the abscissa x , so that the portion of the pore around x is almost deactivated. In this case, the concentration of reactants $C_A(x, t)$ evolves at longer times approximately as

$$C_A(x, t) \approx C_A^{ent} \left[1 - \sqrt{\frac{\tau_0}{2t}} \frac{x}{\ell_c}\right] \quad (38)$$

Distribution of the Activity Along the Pore. Figure 4 shows the behavior of the reactive flux for successive times. When $t \gg \tau_0$, the flux $\phi_A(x, t)$ can be, with very good approximation, written into the following form

$$\phi_A(x, t) = H(t) * F\left(\frac{x - \sqrt{2D_{eff}t}}{\ell_c}\right) \quad (39)$$

with

$$\begin{cases} D_{eff} = \frac{\ell_c^2}{\tau_0} \\ H(t) = \left(\frac{DpC_A^{ent}}{\Lambda_0\sqrt{2}}\right) \sqrt{\frac{\tau_0}{t}} \\ F(u) = \frac{d}{du} [\exp(-g(-u))] \end{cases} \quad (40)$$

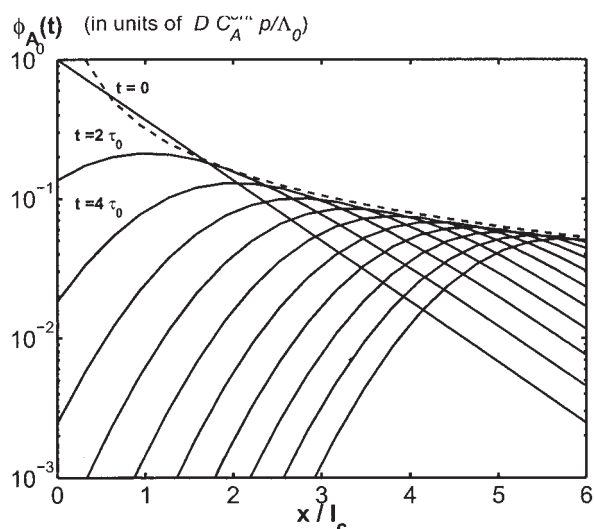


Figure 4. Plots of the chemical activity along a 2-D pore of width w ($p/\sigma = 2/w$), at successive times (every $4\tau_0$).

At the beginning, the chemical activity decreases exponentially in space. When the time t is much larger than τ_0 , the production flux distribution is given by a constant profile, of constant width $2\ell_c$, that progresses into the pore with the square root of time. The envelope $M(x)$ of the profiles, represented by the dashed line, is proportional to the inverse of the abscissa (Eq. 41). The parameter Λ_0 was taken equal to $5w$ in these computations.

This can be analyzed as follows: the total catalytic activity (given by $H(t)$) decreases in time like the inverse of the square root of time as it goes deeper into the pore (Figure 4). Its progression into the pore goes as a classical diffusion law with an effective diffusion constant D_{eff} . Furthermore, the flux of reactants along the pore keeps a constant profile (given by $F(u)$, with $\int_{-\infty}^{+\infty} F(u)du = 1$), with a typical width of order $2\ell_c$. It means that *the size of the active zone remains constant throughout the deactivation of the pore.*

If one transforms the time t in the amplitude $H(t)$ into a space coordinate with the help of the effective diffusion law characterized by D_{eff} , one gets the envelope of the maxima of the chemical flux along the pore (dashed line in Figure 4):

$$M(x) = F(0) * H\left(\frac{x^2}{2D_{eff}}\right) = \left(\frac{2}{e}\right)^{(3/2)} \frac{DpC_A^{ent} \ell_c}{2\Lambda_0 x} \quad (41)$$

The case of prefractal interfaces

In order to investigate the influence of the interface morphology on the production of the catalytic system under deactivation, the response of six different geometries have been studied numerically. As shown in Figure 5, these morphologies correspond to the first six generations of the triangular Von Koch curve.

Each of these diffusion-reaction cells has been discretized in triangular elements, and the solution of the nonlinear Eq. 12 has been computed through finite element techniques.⁴⁰ The profiles displayed in Figure 6 represent the “master curves” of the different cells. The increase of their saturation values (that

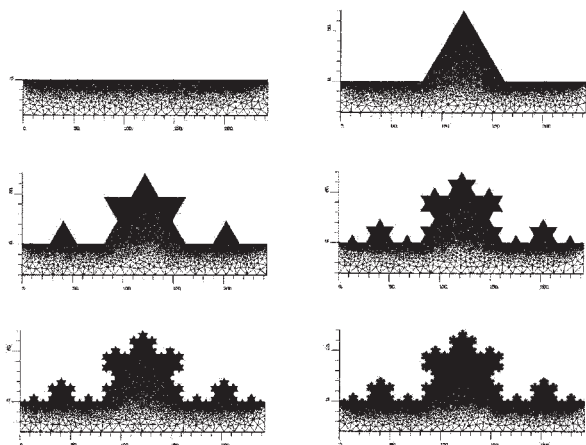


Figure 5. Finite element meshings for the six prefractal interfaces.

is, total production) by a factor of $4/3$ corresponds to the successive values of the fractal perimeters.

Considering the particular case of a constant concentration at the entrance, the dynamical responses of the different catalytic systems can be predicted by direct derivation of the master curve, following Eq. 19. As shown in Figure 6 and Figure 7, from one generation to the next, the increased surface of the catalyst extends the time needed to reach saturation.

The contour plots shown in Figures 8(a)–(d) correspond to the concentration of reactants A (left) and to the diffusion current density (right) for different times. One can see that the activity of the catalytic interface is initially concentrated at the most accessible regions and that this active zone is progressively transferred into the deepest parts of the interface. At the end, the activity is concentrated in the most remote regions of the interface. When, during the deactivation process, the active zone is shifted to a deeper region, this is reflected on the response curve, namely, a marked transition can be observed.

Then, in this type of structure, the catalytic activity starts in the most accessible parts of the interface. Once the first active

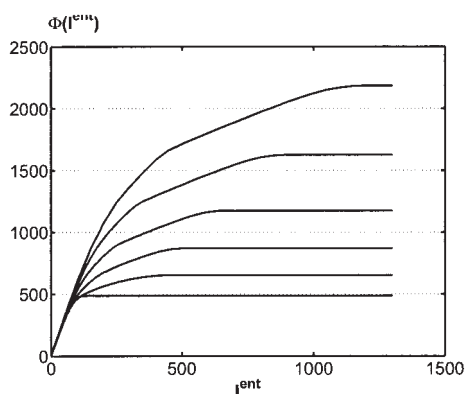


Figure 6. Flux of J^{ent} vs. input concentration J^{ent} for the integrated steady-state system in the six different interfaces.

For each interface, the corresponding curve is the master curve from which the response of the cell for any input concentration $C^{ent}(t)$ can be deduced.

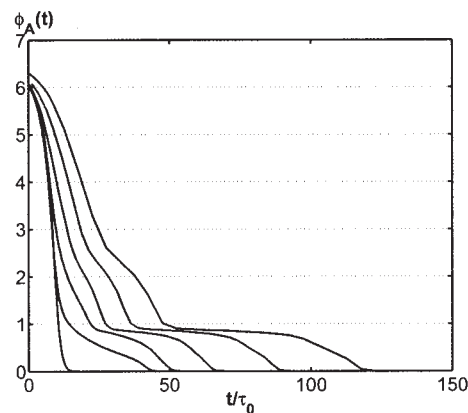


Figure 7. Flux of reactants A vs. time for a constant input concentration C_A^{ent} (obtained by deriving the corresponding master curves as shown in Eq. 19).

The perimeter of the interface at a given generation is exactly $4/3$ times the perimeter of the previous generation. Therefore, the integral of each of these curves is exactly $4/3$ the integral of the previous curve, as demonstrated in Eq. 21.

zone of the catalyst has been exhausted by the fouling reaction, the activity is transferred to the next accessible area. In this new active zone, the production flux is directly determined by the diffusional resistance of access. The process is then repeated up to the point where the entire catalytic surface has

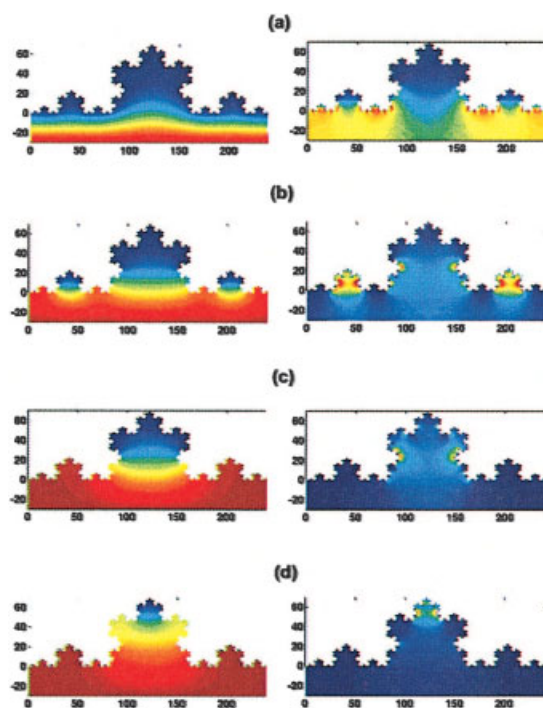


Figure 8. Contour plot of the concentration (left) and the current density (right) of reactant A at various times of the evolution of the catalytic cell: (a) $t/\tau_0 = 10$, (b) $t/\tau_0 = 40$, (c) $t/\tau_0 = 80$, (d) $t/\tau_0 = 130$.

The concentration (left) and current (right) decreases from red to blue.

been deactivated. In the particular case of the prefractal geometry used here, this is revealed by the sequence of shoulders in the response curve, as shown in Figure 7.

Controlling the Time Production of an Unknown Catalyst

As previously demonstrated, the catalytic production under deactivation is fully determined by the function $d\Phi/dI^{ent}$, that is, the derivative of the master curve. Moreover, we have also shown that, even if the geometry of the system and the active sites distribution are unknown, this curve can be experimentally obtained from constant source concentration measurements.

It is important to note that Eq. 16 also provides a way to impose an arbitrary time dependence of the flux $\phi(t)$ through an appropriate (variable) input concentration $C_A^{ent}(t)$. To do so, this concentration must verify

$$C_A^{ent}(t) \left. \frac{d\Phi}{dI^{ent}} \right|_{I^{ent}(t)} = \phi(t) \quad (42)$$

Integrating this equation between 0 and t yields

$$\Phi(I^{ent}(t)) = \int_0^t \phi(\tau) d\tau \equiv F(t)$$

and introducing the inverse function of Φ , Ψ , we finally obtain

$$C_A^{ent}(t) = \frac{d}{dt} [\Psi(F(t))] \quad (43)$$

This equation implies that

$$C_A^{ent}(t) = \phi(t) \left[\left. \frac{d\Phi}{dI^{ent}} \right|_{I^{ent}=\Psi(F(t))} \right]^{-1} \quad (44)$$

In practice, the only requirement is to know $d\Phi/dI^{ent}$, from which Φ and Ψ can be deduced. But as we have shown above this can be deduced from the experimental determination of the behavior of the flux for a constant concentration (or partial pressure) at the entrance of the system.

An important practical problem is to determine how to operate a diffusion-reaction system that is progressively deactivating, in order to obtain a constant flux of product. In mathematical terms, this means that ϕ is constant. Thus, Eq. 44 gives the time-dependence of the concentration needed at the source in order to obtain this constant flux (Figure 9)

$$C_A^{ent}(t) = \phi \left[\left. \frac{d\Phi(I^{ent})}{dI^{ent}} \right|_{I^{ent}=\Psi(\phi t)} \right]^{-1} = \frac{\phi}{\Phi'[\Psi(\phi t)]} \quad (45)$$

We have already seen that the flux Φ of species I saturates at the value

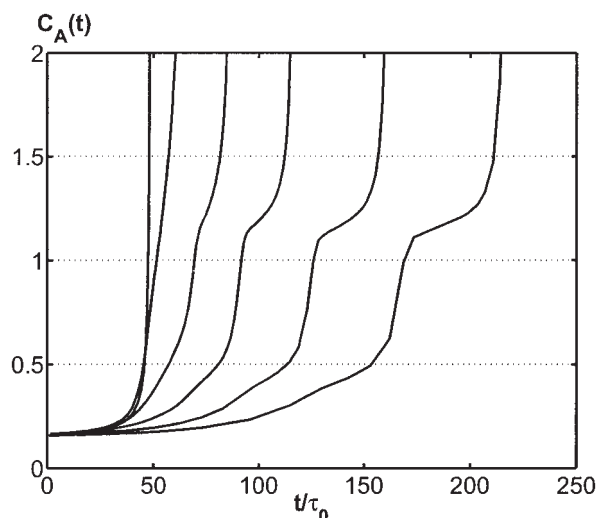


Figure 9. Time evolution of the input concentrations C^{ent} necessary to get a constant flux of products for different generations of the Von Koch interface.

$$\Phi_{sat} = \frac{KC_x^0}{k_2} S_{tot}$$

From this, one can deduce that it is possible to maintain a constant flux of reactants A , f_A , throughout the cell until a time t_{end} such that

$$t_{end} = \frac{KC_x^0}{f_A k_2} S_{tot} \quad (46)$$

Discussion

In this work, the dynamics of deactivation through parallel fouling of an irregular catalytic interface operating under diffusion-limited conditions has been investigated. For the particular case of a first-order reaction, we have been able to develop a general analytical approach to the problem that applies to any arbitrary interface geometry with any distribution of active sites. A few general conclusions can be drawn from this mathematical analysis.

The principal result here is that the behavior of the system, whatever the input concentration and time-dependence, can be deduced from the knowledge of a “master curve.” This curve represents the time integrated production as a function of the time-integrated input concentration. Remarkably, it retains the complete characterization of the catalytic system in terms of its morphology, its diffusional limitations and the chemical reaction kinetics at the surface. On the basis of this method, one can discuss two different scenarios.

First, if the surface geometry and the distribution of active sites is known, the “master curve” can be directly obtained through the numerical solution of the nonlinear problem. An example of this procedure is presented in the section titled “Examples of Catalytic Interfaces,” where the case of diffusion-reaction cells with prefractal catalytic interfaces is analyzed in detail. Using the same approach, the deactivation

process of an infinite pore with smooth walls is investigated analytically. For a constant concentration at the entrance, the production is shown to decay as $t^{-1/2}$. During the deactivation process, the active zone for reaction remains approximately constant in size. This result can be extended to the case of a rough pore with an arbitrary geometry using the tools developed in our previous work.^{20,21}

Second, in the practical case where neither the geometry nor the active sites are known, the method developed here provides a means to obtain the “master curve” from a single experiment, namely, the measure of the time production for a fixed concentration at the input. The master curve can be determined more precisely if one performs several experiments for various input concentrations (or time-dependent profiles). Once obtained, this master curve can be used to predict the dynamics of the system subjected to any input condition. Even more, an arbitrary time production of this (unknown) catalyst can be programmed using these methods. In particular, this can be applied to obtain a constant production flux from a progressively deactivating catalyst.

The role played by the surface geometry on the catalyst performance under slow deactivation and diffusion-limited conditions certainly constitutes an intricate and difficult problem to be solved, both theoretically and experimentally. Clearly, our study represents only one step in this direction, but it relies on a well-defined and systematic approach, that we believe can be experimentally valuable. Besides the mathematical tools developed here, we believe that a general qualitative picture applies to the dynamics of deactivation under diffusion limitations. There should be basically three zones present in the catalyst pellet: (1) a passivated zone which is responsible for diffusional screening; (2) an active zone, where the production takes place, and (3) an still unexploited region, but potentially active. During the dynamics, the passivated zone progressively increases, the size of the active zone remains approximately the same,¹⁷ and the unexploited region decreases. This picture should also apply to higher-order reactions. Our approach also gives some hints on the way to design a catalytic geometry that is proper to a specific chemical process. Although the final total production depends only on the total catalytic surface, we showed here that, as described, the deactivation dynamics can be adequately modulated to perform some required operational task (for example, production at a constant flux).

Acknowledgments

We wish to acknowledge CNPq, CAPES, COFECUB and FUNCAP for financial support.

Notation

$C_A(\vec{x}, t)$	= concentration of reactants A
$C_X(\vec{x}, t)$	= concentration of catalyst X
$C_X^{ent}(t)$	= input concentration of reactants A
$C_X^0(\vec{x})$	= initial concentration of catalyst X
$I(\vec{x}, t)$	= time integrated concentration of reactants A
k_1, k_2, K	= reaction rates ($K = k_1 + k_2$)
D	= molecular diffusion coefficient
$\phi_A(t)$	= flux of reactants A
$\Phi(I^{ent})$	= response of the integrated system (master curve)
$\Psi(\cdot)$	= inverse function of Φ
L	= diameter of the system
L_p	= perimeter of the catalytic interface in 2-D
S_{tot}	= total surface of the catalytic interface in 3-D

Λ_0 = unscreened perimeter length
 τ_D, τ_I = characteristic deactivation times

Literature Cited

1. Aris, R. *The Mathematical Theory of Diffusion and Reaction in Permeable Catalysts*, Clarendon Press, Oxford (1975).
2. Bird, R. B., W. E. Stewart, and E. N. Lightfoot, *Transport Phenomena*, John Wiley & Sons, New York (1960).
3. Adler, P. M., *Porous Media: Geometry and Transport*, Butterworth-Heinemann, Stoneham, MA (1992).
4. Sahimi, M., *Flow and Transport in Porous Media and Fractured Rock*, VCH, Boston (1995).
5. Gavrilo, C., and M. Sheintuch, “Reaction Rates in Fractals vs. Uniform Catalysts with Linear and Nonlinear Kinetics,” *AICHE J.*, **43**, 1691–1699 (1997).
6. Giona, M., “First-Order Reaction-Diffusion Kinetics in Complex Fractal Media,” *Chem. Eng. Sci.*, **47**, 1503–1515 (1992).
7. Gutfraind, R., and M. Sheintuch, “Scaling Approach to Study Diffusion and Reaction Processes on Fractal Catalysts,” *Chem. Eng. Sci.*, **47**, 4425–4433 (1992).
8. Keil, F. J., “Modelling of Phenomena within Catalyst Particles,” *Chem. Eng. Sci.*, **51**, 1543–1567 (1996).
9. McGreavy, C., J. S. Andrade, Jr., and K. Rajagopal, “Consistent Evaluation of Effective Diffusion and Reaction in Pore Networks,” *Chem. Eng. Sci.*, **47**, 2751–2756 (1992).
10. Villermaux, J., D. Schweich, and J.-R. Authelin, “Transfert et réaction à une interface fractale représentée par le ‘Peigne du Diable’,” *C. R. Acad. Sc. Paris Série II*, **304**, 399–404 (1987).
11. Coppens, M.-O., and G. F. Froment, “Diffusion and Reaction in Fractal Catalyst Pore—I. Geometrical Aspects,” *Chem. Eng. Sci.*, **50**, 1013–1026 (1995).
12. Coppens, M.-O., and G. F. Froment, “Diffusion and Reaction in Fractal Catalyst Pore—II. Diffusion and First-Order Reaction,” *Chem. Eng. Sci.*, **50**, 1027–1039 (1995).
13. Coppens, M.-O., “The Effect of Fractal Surface Roughness on Diffusion and Reaction in Porous Catalysts—From Fundamentals to Practical Applications,” *Catalysis Today*, **53**, 225–243 (1999).
14. Meakin, P., “Simulation of the Effects of Fractal Geometry on the Selectivity of Heterogeneous Catalysts,” *Chem. Phys. Lett.*, **123**, 428–432 (1986).
15. Santra, S. B., and B. Sapoval, “Interaction of Ballistic Particles with Irregular Walls, Knudsen Diffusion, and Catalytic Efficiency,” *Phys. Rev. E*, **57**, 6888–6896 (1998).
16. Avnir, D., ed., *The Fractal Approach to Heterogeneous Chemistry: Surfaces, Colloids, Polymers*, Wiley, Chichester (1989).
17. Sapoval, B., “General Formulation of Laplacian Transfer Across Irregular Surfaces,” *Phys. Rev. Lett.*, **73**, 3314–3316 (1994).
18. Pfeifer, P., and B. Sapoval, “Optimization of Diffusive Transport to Irregular Surfaces with Low Sticking Probability,” *Mat. Res. Soc. Symp. Proc.*, **366**, 271–276 (1995).
19. Sapoval, B., “Transport Across Irregular Interfaces: Fractal Electrodes, Membranes and Catalysts,” *Fractals and Disordered Systems*, A. Bunde and S. Havlin, eds., Springer-Verlag, Berlin, pp. 232–261 (1996).
20. Andrade Jr., J. S., M. Filoche, and B. Sapoval, “Analytical Approximation for Diffusion-Reaction Processes in Rough Pores,” *Europhys. Lett.*, **55**, 573–579 (2001).
21. Sapoval, B., J. S. Andrade, Jr., and M. Filoche, “Catalytic Effectiveness of Irregular Interfaces and Rough Pores: The ‘Land Surveyor Approximation’,” *Chem. Eng. Sci.*, **56**, 5011–5023 (2001).
22. Sie, S. T., “Consequences of Catalyst Deactivation for Process Design and Operation,” *Appl. Catal. A*, **212**, 129–151 (2001).
23. Bartholomew, C. H., “Mechanisms of Catalyst Deactivation,” *Appl. Catal. A*, **212**, 17–60 (2001).
24. Moulrijn, J. A., A. E. van Diepen, and F. Kapteijn, “Catalyst Deactivation: Is It Predictable? What To Do?,” *Appl. Catal. A*, **212**, 3–16 (2001).
25. Froment, G. F., “Modeling of Catalyst Deactivation,” *Appl. Catal. A*, **212**, 117–128 (2001).
26. Beeckman, J. W., and G. F. Froment, “Catalyst Deactivation by Active-Site Coverage and Pore Blockage,” *Ind. Eng. Chem. Fund.*, **18**, 245–256 (1979).
27. Beeckman, J. W., and G. F. Froment, “Catalyst Deactivation By Site

- Coverage and Pore Blockage—Finite Rate of Growth of the Carbonaceous Deposit,” *Chem. Eng. Sci.*, **35**, 805–815 (1980).
28. Beeckman, J. W., and G. F. Froment, “Deactivation of Catalysts by Coke Formation in the Presence of Internal Diffusional Limitation,” *Ind. Eng. Chem. Fund.*, **21**, 243–250 (1982).
 29. Nam, I. S., and G. F. Froment, “Catalyst Deactivation by Site Coverage Through Multi-Site Reaction-Mechanisms,” *J. Catal.*, **108**, 271–282 (1987).
 30. Sahimi, M., and T. T. Tsotsis, “A Percolation Model of Catalyst Deactivation by Site Coverage and Pore Blockage,” *J. Catal.*, **96**, 552–562 (1985).
 31. Arbabi, S., and M. Sahimi, “Computer Simulations of Catalyst Deactivation—I. Model Formulation and Validation,” *Chem. Eng. Sci.*, **46**, 1739–1748 (1991).
 32. Arbabi, S., and M. Sahimi, “Computer Simulations of Catalyst Deactivation—II. The Effect of Morphological Transport and Kinetic Parameters on the Performance of the Catalyst,” *Chem. Eng. Sci.*, **46**, 1749–1755 (1991).
 33. Malek, K., and M.-O. Coppens, “Effects of Surface Roughness on Self- and Transport Diffusion in Porous Media in the Knudsen Regime,” *Phys. Rev. Lett.*, **87**, 125505 (2001).
 34. Andrade Jr., J. S., H. F. da Silva, M. Baquil, and B. Sapoval, “Transition from Knudsen to Molecular Diffusion in Activity of Absorbing Irregular Interfaces,” *Phys. Rev. E*, **68**, 41608 (2003).
 35. Filoche, M., and B. Sapoval, “A Simple Method to Compute the Response of Non-Homogeneous and Irregular Interfaces: Electrodes and Membranes,” *J. Phys. I France*, **7**, 1487–1498 (1997).
 36. Jones, P., and T. Wolff, “Hausdorff Dimension of Harmonic Measures in the Plane,” *Acta Math.*, **161**, 131–144 (1988).
 37. Makarov, N. G., “On the Distortion of Boundary Sets Under Conformal Mapping,” *Proc. London Math. Soc.*, **51**, 369–384 (1985).
 38. Filoche, M., and B. Sapoval, “Shape Dependence of the Non-Linear Response of Irregular Electrodes,” *Electrochimica Acta*, **46**, 213–220 (2000).
 39. Sapoval, B., M. Filoche, K. Karamanos, and R. Brizzi, “Can One Hear the Shape of an Electrode? I. Numerical Study of the Active Zone in Laplacian Transfer,” *Eur. Phys. J. B.*, **9**, 739–753 (1999).
 40. Bernadou, M. et al., “Modulef: Une Bibliothèque Modulaire d’Éléments finis,” *INRIA Report*, France (1985).

Manuscript received Nov. 14, 2003, and revision received July 9, 2004.